

Jet launching theory and the vertical structure of a magnetically-dominated thin accretion disc

G. Rüdiger¹ and D. Shalybkov^{1,2}

¹ *Astrophysikalisches Institut Potsdam, An der Sternwarte 16, D-14482 Potsdam, Germany*
gruediger@aip.de

² *A.F. Ioffe Institute for Physics and Technology, 194021, St. Petersburg, Russia*
dasha@astro.ioffe.rssi.ru

12 February 2022

ABSTRACT

The presence of an imposed external magnetic field may drastically influence the structure of thin accretion discs. The magnetic field energy is here assumed to be in balance with the thermal energy of the accretion flow. The vertical magnetic field, its toroidal component B^{tor} at the disc surface (due to different rotation rates between disc and its magnetosphere), the turbulent magnetic Prandtl number and the viscosity-alpha are the key parameters of our model. Inside the corotation radius for rather small B^{tor} the resulting inclination angle i of the magnetic field lines to the disc surface normal can exceed the critical value 30° (required to launch cold jets) even for small magnetic Prandtl numbers of order unity. The self-consistent consideration of both magnetic field and accretion flow demonstrates a weak dependence of the inclination (“dragging”) angle on the magnetic Prandtl number for given surface density but a strong dependence on the toroidal field component at the disc surface.

A magnetic disc is thicker than a nonmagnetic one for typical parameter values. The accretion rate can be strongly amplified by large B^{tor} and small magnetic Prandtl number. On the other hand, for given accretion rate the magnetised disc is less massive than the standard-alpha disc. The surface values of the toroidal magnetic fields which are necessary to induce considerably high values for the inclination angle are much smaller than expected and are of order 10^{-3} of the imposed vertical field. As the innermost part of the disc produces the largest B^{tor} , the largest radial inclination can be expected also there. The idea is therefore supported that the cold jets are launched only in the central disc area.

Key words: accretion, accretion discs – magnetic fields – MHD

1 INTRODUCTION

Accretion flows is assumed to occur in a variety of astrophysical objects. The structure of magnetic accretion discs is the problem of major importance, for example, for understanding of the origin of astrophysical jets. If the inclination, i , of the field lines from the vertical exceeds 30° , the plasma can be accelerated when spiralling along the field line (Blandford & Payne 1982; Lynden-Bell 1996; Campbell 1997; Krasnopolsky, Li & Blandford 1999). Accretion disc-driven magnetocentrifugal winds have been widely used to model the astrophysical jets (e.g. Ustyugova et al. 1999, Ouyed & Pudritz 1999, Krasnopolsky, Li & Blandford 1999).

The present study is motivated by a series of papers dealing with the interaction of accretion discs with external magnetic fields (Livio & Pringle 1992; Lubow, Papaloizou & Pringle 1994; Bardou & Heyvaerts 1996; Reyes-Ruiz &

Stepinski 1996; Ogilvie 1997; Ogilvie & Livio 1998; Campbell 1998; Campbell & Heptinstall 1998a, 1998b; Brandenburg & Campbell 1998). In the presence of a vertical magnetic field, the vertical gradient of angular velocity generates the toroidal field due to the stretching effect. This field may generally influence the vertical and radial structure of a disc and alter the angular momentum transport. If the magnetic field is sufficiently strong it even will influence the rotation law (Ogilvie 1997; Ogilvie & Livio 1998).

Our previous paper (Shalybkov & Rüdiger 2000, hereafter paper I) considered the self-consistent steady-state structure of the polytropic accretion disc in the presence of a vertical magnetic field. In the present paper we will refuse from simplified polytropic equation of state and solve the full system of MHD equations for the vertical accretion disc structure. So better comparisons with the theory of the vertical structure of accretion discs without magnetic field are

possible. As known, such computations, for given viscosity-alpha and given opacity law, yield the accretion rate \dot{M} for any possible column density Σ . The same is done here for an accretion disc threaded by a magnetic field with a given vertical component B^{vert} and a given toroidal component B^{tor} which, of course, have opposite signs if we are within the corotation radius^{*}. Such a configuration can only exist for a certain accretion rate and with a certain distribution of a radial magnetic field component B_R . The value of the latter taken at the surface defines the inclination angle i known from the jet theory. Along this way the well-known dragging problem – to find the radial inclination i – has been unified with the theory of the vertical structure of accretion discs.

There is an estimate for the toroidal component B^{tor} due to the different rotation of halo and disc. If a disc halo with a high conductivity exists then the surface value of B_ϕ will become large. After Campbell (1992) the shear between the rigidly rotating halo and the accretion disc induces a toroidal magnetic field of

$$B^{\text{tor}} = -\gamma \frac{R}{H} \frac{\text{Pm}}{\alpha_{\text{SS}}} \frac{\Omega_{\text{Kep}} - \Omega_*}{\Omega_{\text{Kep}}} B^{\text{vert}} \quad (1)$$

with Ω_* as the stellar rotation rate. The numerical integration of the induction equation for a uniform and a dipolar field and a plasma halo (with conductivity of 10 times of the disc conductivity) confirms this result with $\gamma \simeq 1$ (Elstner & Rüdiger 2000). The toroidal surface field changes its sign at the corotation radius where Ω_{Kep} equals the stellar rotation rate Ω_* . The magnetic torque results as negative inside the corotation radius and positive outside the corotation radius. For a disc embedded in vacuum, of course, the γ in (1) vanishes. We consider the γ as representing the unknown halo conductivity. We shall show here that we only need very small γ in order to produce inclination angles i of the interesting value of 30° and more – independent of the the magnetic Prandtl number Pm . We also can take from (1) and from the simulations by Elstner & Rüdiger that the ratio

$$\beta = \frac{B^{\text{tor}}}{B^{\text{vert}}} \quad (2)$$

– which is negative (positive) inside (outside) the corotation radius grows (by absolute value) inwards. This fact will play an important role in the philosophy of the presented research.

2 BASIC EQUATIONS

Consider the structure of an axisymmetric disc in a steady-state regime; R , ϕ , and z are the cylindrical coordinates. The resulting kinetic and magnetic equations are given in paper I as the Eqs. (1)...(13) there. Here we have only to add the energy equation. All generated energy is assumed to be transferred from the disc by radiation neglecting convection, and the disc is optically thick. Then the energy equation is

$$\frac{1}{R} \frac{\partial}{\partial R} (R F_R) + \frac{\partial F_z}{\partial z} = \rho \nu \left[2 \left(\frac{\partial u_R}{\partial R} \right)^2 + 2 \left(\frac{u_R}{R} \right)^2 + \right.$$

$$\left. + 2 \left(\frac{\partial u_z}{\partial z} \right)^2 + \left(R \frac{\partial}{\partial R} \left(\frac{u_\phi}{R} \right) \right)^2 + \right. \\ \left. + \left(\frac{\partial u_\phi}{\partial z} \right)^2 + \left(\frac{\partial u_R}{\partial z} + \frac{\partial u_z}{\partial R} \right)^2 - \right. \\ \left. - \frac{2}{3} \left(\frac{1}{R} \frac{\partial}{\partial R} (R u_R) + \frac{\partial u_z}{\partial z} \right)^2 \right] + \frac{\eta_T}{\mu_0} \left[\left(\frac{\partial B_\phi}{\partial z} \right)^2 + \right. \\ \left. + \left(\frac{\partial B_R}{\partial z} - \frac{\partial B_z}{\partial R} \right)^2 + \left(\frac{1}{R} \frac{\partial}{\partial R} (R B_\phi) \right)^2 \right], \quad (3)$$

where the energy flux components are

$$F_R = -\frac{16\sigma T^3}{3\kappa\rho} \frac{\partial T}{\partial R}, \quad F_z = -\frac{16\sigma T^3}{3\kappa\rho} \frac{\partial T}{\partial z} \quad (4)$$

with σ is the Stefan-Boltzmann constant, T is the temperature and κ the Roseland mean opacity.

The equations must be supplemented by relations specifying the gravitational potential, the equation of state, the opacity, the viscosity, and the magnetic diffusivity. We neglect the self-gravitation of the disc so that

$$\psi = -\frac{GM_*}{(R^2 + z^2)^{1/2}}, \quad (5)$$

where G is the gravity constant and M_* is the mass of the central object. We adopt here the ideal-gas equation of state $P = \mathcal{R}\rho T/\mu$ (\mathcal{R} is the molar gas constant and μ is the mean molecular mass) and the opacity may fulfil a power law, $\kappa = k_0 \rho^\gamma T^\delta$, with the constant quantities k_0 , γ and δ . This includes the cases of Thomson scattering opacity ($k_0 \approx 0.4$, $\gamma = \delta = 0$) and Kramers opacity ($k_0 \approx 6.6 \cdot 10^{22}$, $\gamma = 1$, $\delta = -3.5$). A Shakura-Sunyaev parameterisation is used for the turbulent viscosity,

$$\rho \nu_T = \alpha_{\text{SS}} \frac{P}{\Omega}, \quad (6)$$

where α_{SS} is a constant (Shakura & Sunyaev 1973). For the magnetic diffusivity we assume that the magnetic Prandtl number $\text{Pm} = \nu_T/\eta_T$ is constant.

Following Regev (1983) and Kluzniak & Kita (2000) we scale all quantities by their correspondent characteristic values. This will make the equations dimensionless and allows to compare the relative significances of each term. The radial distances are scaled by some characteristic radius, \tilde{R} , and vertical distances by a typical vertical height of the disc, \tilde{H} . We represent the angular velocity in units of the Keplerian velocity at the characteristic radius, $\tilde{\Omega}^2 = GM_*/\tilde{R}^3$. Using these three characteristic quantities all others can be defined. The typical sound speed is $\tilde{c}_s = \tilde{H}\tilde{\Omega}$, the typical viscosity and magnetic diffusivity $\tilde{\nu} = \tilde{\eta} = \tilde{c}_s\tilde{H}$, the typical temperature is $\tilde{T} = \mu/\mathcal{R}\tilde{c}_s^2$, the typical pressure is $\tilde{P} = \tilde{\rho}\tilde{c}_s^2$, the typical energy flux is $\tilde{F} = \tilde{\rho}\tilde{c}_s^3$, and the typical magnetic field is $\tilde{B} = (\mu_0\tilde{\rho})^{1/2}\tilde{c}_s$. The last three quantities use typical density, $\tilde{\rho}$, which transforms the equation for the vertical energy flux to the dimensionless form, i.e.

$$\tilde{\rho} = \left(\frac{16\sigma}{3k_0} \tilde{H}^{4-2\delta} \tilde{\Omega}^{5-2\delta} \left(\frac{\mu}{\mathcal{R}} \right)^{4-\delta} \right)^{\frac{1}{\gamma+2}}. \quad (7)$$

Note that the typical magnetic field defined above \tilde{B} gives $\tilde{V}_A = \tilde{B}/(\mu_0\tilde{\rho})^{1/2} \equiv \tilde{c}_s$, where \tilde{V}_A is the typical Alfvén velocity. The last relation defines the magnetic field energy as in balance with the accretion flow energy. The dimensionless equation of state takes the simple form $P = \rho T$, where

^{*} At the corotation radius the component B^{tor} vanishes; for a nonrotating central object the corotation radius is in the infinity

the same symbols as before are used for the dimensionless quantities.

Let us define the parameter ϵ

$$\epsilon = \tilde{H}/\tilde{R} = V_A/\tilde{\Omega}\tilde{R}. \quad (8)$$

As in paper I we consider a geometrically thin disc ($\epsilon \ll 1$) and expand all variables in power of ϵ , i.e.

$$A(R, z) = A_0(R, z) + \epsilon A_1(R, z) + \dots$$

Using the same symbols for the normalized quantities, the full system at the leading order of ϵ takes the form

$$u_{R0}B^{\text{vert}} + \eta_{T0}\frac{\partial B_{R0}}{\partial z} = 0, \quad (9)$$

$$RB^{\text{vert}}\frac{\partial \Omega_1}{\partial z} + RB_{R0}\frac{\partial \Omega_0}{\partial R} + \frac{\partial}{\partial z}\left(\eta_{T0}\frac{\partial B_{\phi 0}}{\partial z}\right) = 0, \quad (10)$$

$$-2\rho_0\Omega_0\Omega_1R = B^{\text{vert}}\frac{\partial B_{R0}}{\partial z} + \frac{\partial}{\partial z}\left(\rho_0\nu_{T0}\frac{\partial u_{R0}}{\partial z}\right), \quad (11)$$

$$\rho_0\frac{u_{R0}}{R}\frac{\partial}{\partial R}(R^2\Omega_0) = B^{\text{vert}}\frac{\partial B_{\phi 0}}{\partial z} + \frac{\partial}{\partial z}\left(\rho_0\nu_{T0}R\frac{\partial \Omega_1}{\partial z}\right), \quad (12)$$

$$\frac{\partial P_0}{\partial z} + \rho_0\frac{z}{R^3} + B_{\phi 0}\frac{\partial B_{\phi 0}}{\partial z} + B_{R0}\frac{\partial B_{R0}}{\partial z} = 0, \quad (13)$$

$$\begin{aligned} \frac{\partial F_0}{\partial z} = & \rho_0\nu_{T0}\left[\left(R\frac{\partial \Omega_0}{\partial R}\right)^2 + \left(R\frac{\partial \Omega_1}{\partial z}\right)^2 + \left(\frac{\partial u_{R0}}{\partial z}\right)^2\right] + \\ & + \eta_{T0}\left[\left(\frac{\partial B_{\phi 0}}{\partial z}\right)^2 + \left(\frac{\partial B_{R0}}{\partial z}\right)^2\right] \end{aligned} \quad (14)$$

and

$$F_0 = -\frac{T_0^{3-\delta}}{\rho_0^{1+\gamma}}\frac{\partial T}{\partial z}, \quad (15)$$

where $B_{z0} \equiv B^{\text{vert}}$ and $\Omega_0 = R^{-3/2}$ is the normalized Keplerian velocity. Equations (9)....(13) are identic with those of paper I. Note that after (14) and (15) all energy is assumed to be transported in the vertical direction.

The system (9)....(15) depends on R only as parameter and we can use the real radius R as scaling constant \tilde{R} , the real disc half-thickness H as scaling constant \tilde{H} and the real Keplerian angular velocity $\Omega_{\text{Kep}} = \sqrt{GM_*/R^3}$ as scaling constant $\tilde{\Omega}$. The system takes thus the final form

$$u_R B^{\text{vert}} + \frac{\alpha_{\text{SS}}}{\text{Pm}} T \frac{\partial B_R}{\partial z} = 0, \quad (16)$$

$$B^{\text{vert}}\frac{\partial u_\phi}{\partial z} - \frac{3}{2}B_R + \frac{\alpha_{\text{SS}}}{\text{Pm}}\frac{\partial}{\partial z}\left(T\frac{\partial B_\phi}{\partial z}\right) = 0, \quad (17)$$

$$-2\frac{P}{T}u_\phi = B^{\text{vert}}\frac{\partial B_R}{\partial z} + \alpha_{\text{SS}}\frac{\partial}{\partial z}\left(P\frac{\partial u_R}{\partial z}\right), \quad (18)$$

$$0.5\frac{P}{T}u_R = B^{\text{vert}}\frac{\partial B_\phi}{\partial z} + \alpha_{\text{SS}}\frac{\partial}{\partial z}\left(P\frac{\partial u_\phi}{\partial z}\right), \quad (19)$$

$$\frac{\partial P}{\partial z} + \frac{P}{T}z + B_\phi\frac{\partial B_\phi}{\partial z} + B_R\frac{\partial B_R}{\partial z} = 0, \quad (20)$$

$$\begin{aligned} \frac{\partial F}{\partial z} = & \alpha_{\text{SS}}P\left[\frac{9}{4} + \left(\frac{\partial u_\phi}{\partial z}\right)^2 + \left(\frac{\partial u_R}{\partial z}\right)^2\right] + \\ & + \frac{\alpha_{\text{SS}}}{\text{Pm}}T\left[\left(\frac{\partial B_\phi}{\partial z}\right)^2 + \left(\frac{\partial B_R}{\partial z}\right)^2\right] \end{aligned} \quad (21)$$

and

$$F = -\frac{T^{4-\delta+\gamma}}{P^{1+\gamma}}\frac{\partial T}{\partial z}, \quad (22)$$

if also the suffices 0 and 1 are dropped. These relations form a nonlinear set of differential equations for P , T , F , u_R , u_ϕ , B_R , B_ϕ with α_{SS} , Pm , and B^{vert} as parameters. There are also two implicit parameters, i.e. R and the central mass M_* . Solving the equations for given R and M_* the vertical structure for given α_{SS} , Pm and B^{vert} is found with 10 reasonable boundary conditions.

For discs symmetric with respect to the midplane ($z = 0$) the physical quantities such as Ω , u_R , T are even functions of z while B_R , B_ϕ , F are odd functions of z . Such symmetries provide the boundary conditions at the midplane ($z = 0$) as

$$B_R = B_\phi = \partial u_R/\partial z = \partial u_\phi/\partial z = F = 0. \quad (23)$$

At the disc surface, $z = 1$, it no external pressure is allowed. The simplest boundary condition for the temperature, $T(1) = 0$, is used. It reflects the fact that for optically thick disc the surface temperature must be much smaller than the temperature at the disc midplane. Then the first of the above equations immediately gives $u_R(1) = 0$ for $T(1) = 0$. We additionally fix the toroidal and vertical magnetic field at the surface as the last two boundary conditions. It means that the angle β is fixed and also the accretion rate (see (26) and (35)). Hence, the boundary conditions at $z = 1$ are

$$P = T = u_R = 0, \quad B_\phi = B^{\text{tor}}, \quad B_z = B^{\text{vert}}, \quad (24)$$

where B^{tor} and B^{vert} are free constants. As usual in the theory of the vertical structure of accretion discs, the accretion rate (or the column density Σ) remain the only free parameter.

3 PHYSICAL PARAMETERS

It is useful to connect our normalized quantities with the real physical values. The real physical parameters of the problem are the distance to the central object, R , its mass M_* , the accretion rate \dot{M} and the inclination angle i of the magnetic field lines to the rotation axis. Note that we can choose any of the accretion rate, the surface density and the disc half-thickness as the free parameter of the problem. All these quantities are connected with each other (see below). Accretion rate is more convenient as a parameter from the physical point of view, but the disc half-thickness is more natural for numerical calculations.

The accretion rate \dot{M} and the surface density Σ as functions of half-thickness H are

$$\dot{M} = 4\pi R \tilde{\rho} \tilde{c}_s H \hat{M}, \quad (25)$$

where the $\tilde{\rho}$ is given by (7) and the normalized accretion rate \hat{M} is

$$\hat{M} = -\int_0^1 u_{R0} \rho_0 dz \quad (26)$$

and

$$\Sigma = 2\tilde{\rho}H\hat{\Sigma}, \quad (27)$$

where the normalized surface density is

$$\hat{\Sigma} = \int_0^1 \rho_0 dz. \quad (28)$$

The disc thickness and the surface density as functions of \dot{M} are

$$H = \left(\frac{3k_0}{16\sigma} \left(\frac{\mathcal{R}}{\mu} \right)^{4-\delta} \Omega_{\text{Kep}}^{2\delta-7-\gamma} \left(\frac{\dot{M}\epsilon}{4\pi\hat{M}} \right)^{\gamma+2} \right)^{\frac{1}{10-2\delta+3\gamma}}, \quad (29)$$

where the ϵ after (8) is

$$\epsilon = \left(R^{2\delta-10-3\gamma} \frac{3k_0}{16\sigma} \left(\frac{\mathcal{R}}{\mu} \right)^{4-\delta} \Omega_{\text{Kep}}^{2\delta-7-\gamma} \left(\frac{\dot{M}}{4\pi\hat{M}} \right)^{\gamma+2} \right)^{\frac{1}{8-2\delta+2\gamma}} \quad (30)$$

and the surface density

$$\Sigma = 2\hat{\Sigma} \left(\left(\frac{16\sigma}{3k_0} \left(\frac{\mu}{\mathcal{R}} \right)^{4-\delta} \right)^2 \Omega_{\text{Kep}}^{4-2\delta-\gamma} \left(\frac{\dot{M}\epsilon}{4\pi\hat{M}} \right)^{6-2\delta+3\gamma} \right)^{\frac{1}{10-2\delta+3\gamma}}. \quad (31)$$

Half-thickness and accretion rate as functions of Σ are

$$H = \left(\frac{3k_0}{16\sigma} \left(\frac{\mathcal{R}}{\mu} \right)^{4-\delta} \Omega_{\text{Kep}}^{2\delta-5} \left(\frac{\Sigma}{2\hat{\Sigma}} \right)^{2+\gamma} \right)^{\frac{1}{6+\gamma-2\delta}} \quad (32)$$

and

$$\dot{M} = 4\pi R^2 \epsilon \Omega_{\text{Kep}} \Sigma \frac{\hat{M}}{2\hat{\Sigma}} \quad (33)$$

with

$$\epsilon = \frac{1}{R} \left(\frac{3k_0}{16\sigma} \left(\frac{\Sigma}{2\hat{\Sigma}} \right)^{2+\gamma} \left(\frac{\mathcal{R}}{\mu} \right)^{4-\delta} \Omega_{\text{Kep}}^{2\delta-5} \right)^{\frac{1}{6+\gamma-2\delta}}. \quad (34)$$

Integrating Eq. (19) over z one finds

$$\int_0^1 \rho u_R dz = 2B^{\text{vert}} B^{\text{tor}}, \quad (35)$$

so that (25) turns into

$$\dot{M} = -8\pi R \tilde{\rho} \tilde{c}_s H B^{\text{vert}} B^{\text{tor}}. \quad (36)$$

The accretion is thus provided by the surface toroidal magnetic field in our model in strong contrast to the standard-alpha disc theory. According to the latter, the surface density Σ_0 of the disc is $\Sigma_0 = \dot{M}/3\pi\nu$ with $\nu = 2\alpha_{\text{SS}} c_s H_0$ and $c_s = 2H_0 \Omega_{\text{Kep}}$, where \dot{M} and H_0 are the accretion rate and the disc half-thickness without a magnetic field.[†] The Σ_0 and H_0 as functions M_* , R and \dot{M} are

$$H_0 = \frac{1}{2} \left(\frac{9}{32\pi(3\pi\alpha_{\text{SS}})^{1+\gamma}} \frac{k_0}{\sigma} \dot{M}^{2+\gamma} \Omega_{\text{Kep}}^{2\delta-7-\gamma} \left(\frac{\mathcal{R}}{\mu} \right)^{4-\delta} \right)^{\frac{1}{10-2\delta+3\gamma}} \quad (37)$$

$$\Sigma_0 = \frac{1}{3\pi} \left(\left(\frac{32\pi(3\pi)^{1+\gamma}}{9} \frac{\sigma}{k_0} \right)^2 \alpha_{\text{SS}}^{2\delta-8-\gamma} \dot{M}^{6-2\delta+\gamma} \Omega_{\text{Kep}}^{4-2\delta-\gamma} \right)$$

[†] We shall always neglect the factor $1 - (R_*/R)^{1/2}$ with R_* as the central object radius.

$$\left(\frac{\mu}{\mathcal{R}} \right)^{8-2\delta} \right)^{\frac{1}{10-2\delta+3\gamma}}. \quad (38)$$

We are here interested to know the magnetic influence on the accretion rate, the disc height and the surface density. We shall consider two ratios for each quantities, for given accretion rate or for given surface density, resp.. Nevertheless, all these characteristics are related to each other, and consideration of one ratio is sufficient. For given accretion rate, it results

$$\frac{H}{H_0} = 2 \left(\frac{2\pi(3\pi\alpha_{\text{SS}})^{1+\gamma}}{3} \left(\frac{\epsilon}{4\pi\hat{M}} \right)^{\gamma+2} \right)^{\frac{1}{10-2\delta+3\gamma}}, \quad (39)$$

$$\frac{\Sigma}{\Sigma_0} = 2\hat{\Sigma} \left(\frac{9}{4\pi^2(3\pi)^{2\gamma+2}} \alpha_{\text{SS}}^{8-2\delta+\gamma} \left(\frac{\epsilon}{4\pi\hat{M}} \right)^{6-2\delta+\gamma} \right)^{\frac{1}{10-2\delta+3\gamma}} \quad (40)$$

and for given surface density

$$\Psi = \frac{\dot{M}}{M_0} = \frac{4}{3\epsilon} \hat{M} \left(\frac{4}{81} \alpha_{\text{SS}}^{2\delta-8-\gamma} (2\hat{\Sigma})^{2\delta-10-3\gamma} \right)^{\frac{1}{6-2\delta+\gamma}}. \quad (41)$$

Our calculations will reveal the latter quantity always exceeding unity so that for given column density Σ the related accretion rate \dot{M} is higher for magnetised disc; and for given accretion rate the related column density is smaller than without magnetic field.

The Mach number of the radial flow is

$$\text{Ma} = \frac{u_R}{c_s} = \left(\frac{3}{5} \right)^{1/2} \frac{u_R}{T^{1/2}}, \quad (42)$$

where we have used the ideal gas sound speed $c_s^2 = 5/3 P/\rho$.

The inclination angle i of the radial magnetic field component at the surface B_{Rs} to the rotation axis is

$$\tan i = \frac{B_{Rs}}{B^{\text{vert}}}. \quad (43)$$

Its determination for prescribed accretion rate is the central point of the present paper, the often formulated dragging problem corresponds to the theory of the vertical structure of accretion discs in external magnetic fields.

Below we shall use the constants $R = 10^{10} \text{ cm}$, $M_* = 1M_\odot$, $\mu = 6.6 \cdot 10^{22}$, $\gamma = 1$, $\delta = -7/2$. The Kepler velocity is $\Omega_{\text{Kep}} = 1.2 \cdot 10^{-2} \text{ s}^{-1}$. The normalisation constants with $\epsilon = 0.01$ as a typical value[‡] are $\tilde{\rho} = 2.8 \cdot 10^{-8} \text{ g/cm}^3$, $\tilde{c}_s = 1.1 \cdot 10^6 \text{ cm/s}$, $\tilde{T} = 8.7 \cdot 10^3 \text{ K}$, $\tilde{\nu} = \tilde{\eta} = 1.1 \cdot 10^{14} \text{ cm}^2/\text{s}$, $\tilde{F} = 3.7 \cdot 10^{10} \text{ erg cm}^{-2} \text{ s}^{-1}$ and the unit for the magnetic field is $\tilde{B} = 590 \text{ G}$.

4 RESULTS AND DISCUSSION

The systems of ordinary differential equations (16)...(22) with boundary conditions (23) and (24) are solved by a relaxation method (see Press et al. 1992). The dependent variables are P , T , F , u_R , u_ϕ , B_R , and B_ϕ . The parameters are α_{SS} , Pm , \dot{M} , B^{vert} and B^{tor} . Only Kramers opacity is used.

[‡] It can be easily calculated according to (30) or (34) and models values specified above and in Table 1.

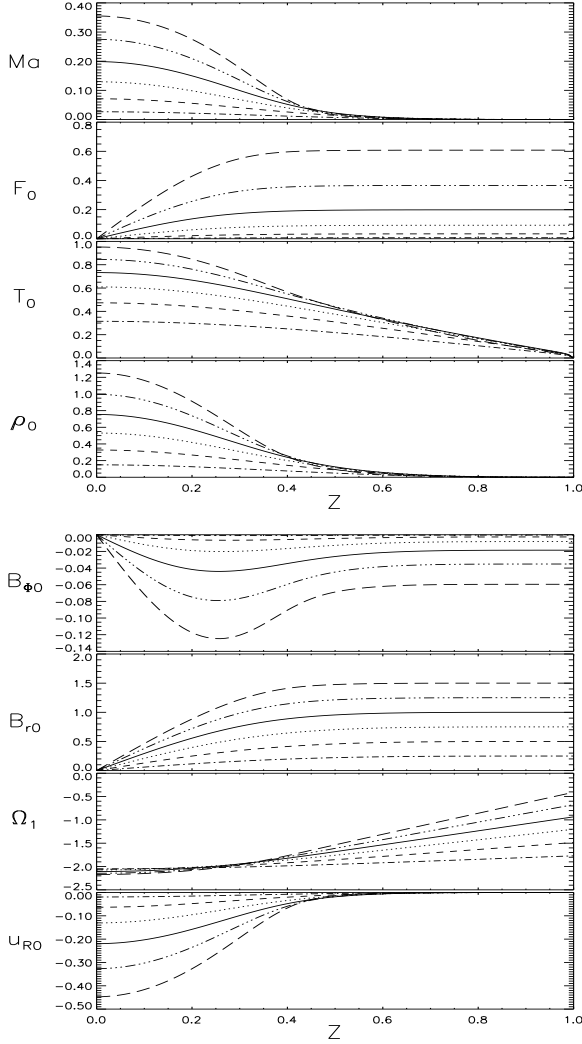


Figure 1. The vertical disc structure for $\alpha_{SS} = 0.1$, $Pm = 1$ and $B^{vert} = 1$. The β is $-4 \cdot 10^{-4}$ (dot-dashed), $-2.6 \cdot 10^{-3}$ (short-dashed), $-8.2 \cdot 10^{-3}$ (dotted), $-1.9 \cdot 10^{-2}$ (solid), $-3.5 \cdot 10^{-2}$ (dot-dot-dot-dashed), $-5.1 \cdot 10^{-2}$ (long-dashed). The values of \hat{M} , $\hat{\Sigma}$ and i for each curve are given in Table 1

The calculation demonstrated that for a fixed B^{tor} one always can adjust B_{Rs} to fulfil the condition (35). On the other hand, for fixed B_{Rs} there is some critical value of the α_{SS} for given Pm , B^{vert} and B^{tor} fixed by (35). It was possible to find the solution only for $\alpha_{SS} < \alpha_{cr}$. The $\alpha_{cr} \approx 0.4$ for $Pm = 1$, $B^{vert} = 1$ and $B_{Rs} = 1$. Due to the nonlinear character of the system the reasons for this numerical problems are difficult to understand. Nevertheless, the real physical interest requires calculations with $\alpha_{SS} < 1$. We have restricted ourselves to calculations for $\alpha_{SS} \leq 0.1$ only.

The vertical disc structure is illustrated in Figs. 1 and 2. We performed the calculations for vertical disc structure as function of Pm and B^{vert} for one of three parameters (\hat{M} , $\hat{\Sigma}$ and i) fixed. Two values of viscosity-alpha, i.e. $\alpha_{SS} = 0.01$ and $\alpha_{SS} = 0.1$, are used always. The qualitative behaviour of the solutions is very similar for both cases. The profiles in Figs. 1 and 2 are labelled by the toroidal inclination β . We could them also label either with the nondimensional

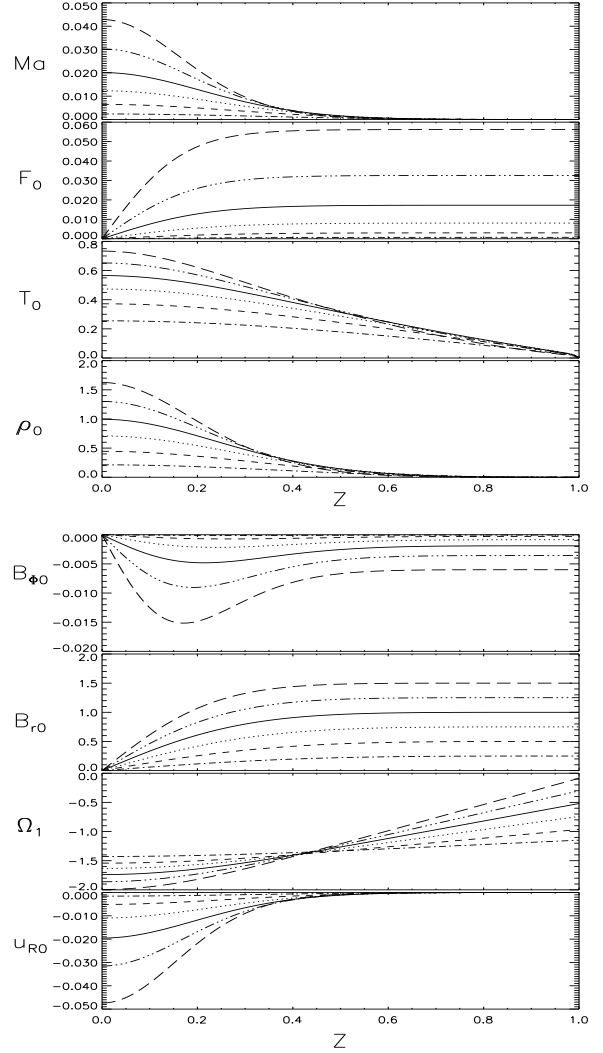


Figure 2. The same as on Fig.1, but for $\alpha_{SS} = 0.01$

accretion rate \hat{M} or the nondimensional surface density $\hat{\Sigma}$ according to Table 1.

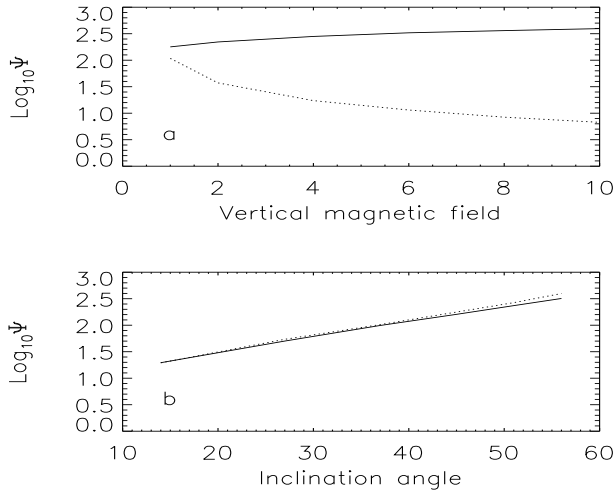
Almost the entire variation of the disc variables happens for $0 < z < 0.5$ hence always we have ‘atmospheres’ for $z > 0.5$. The atmosphere becomes thinner for increasing values of the vertical field. The flow is subsonic ($Ma < 1$) and the applied surface toroidal magnetic field is much smaller in comparison with B^{vert} ($|\beta| \leq 0.1$) for all calculated cases. The density and the temperature weakly depend on the turbulence parameters α_{SS} and Pm for large α_{SS} . The accretion flow at the disc midplane can be comparable with the sound velocity. However, due to the weak dependence of the temperature on α_{SS} , the Mach number behaves almost linear with α_{SS} and therefore $Ma \ll 1$ for $\alpha_{SS} \ll 1$.

4.1 Accretion rate and surface density

The accretion rate for magnetic discs drastically increases in comparison with nonmagnetic discs (see Figs. 3 and 4). Nevertheless, the accretion rate for magnetic discs can be even smaller than for nonmagnetic discs for large Pm and

Table 1. The model parameters ($Pm = 1$, $B^{\text{vert}} = 1$)

α_{SS}	β	i	\dot{M}	$\hat{\Sigma}$
0.1	$-4.0 \cdot 10^{-4}$	14°	$8.0 \cdot 10^{-4}$	0.062
0.1	$-2.6 \cdot 10^{-3}$	27°	$5.2 \cdot 10^{-3}$	0.13
0.1	$-8.2 \cdot 10^{-3}$	37°	0.016	0.19
0.1	$-1.9 \cdot 10^{-2}$	45°	0.037	0.25
0.1	$-3.5 \cdot 10^{-2}$	51°	0.070	0.31
0.1	$-5.9 \cdot 10^{-2}$	56°	0.12	0.37
0.01	$-4.7 \cdot 10^{-5}$	14°	$9.3 \cdot 10^{-5}$	0.090
0.01	$-2.8 \cdot 10^{-4}$	27°	$5.6 \cdot 10^{-4}$	0.17
0.01	$-8.5 \cdot 10^{-4}$	37°	$1.7 \cdot 10^{-3}$	0.25
0.01	$-1.9 \cdot 10^{-3}$	45°	$3.8 \cdot 10^{-3}$	0.31
0.01	$-3.6 \cdot 10^{-3}$	51°	$7.1 \cdot 10^{-3}$	0.37
0.01	$-6.0 \cdot 10^{-3}$	56°	$1.2 \cdot 10^{-2}$	0.41

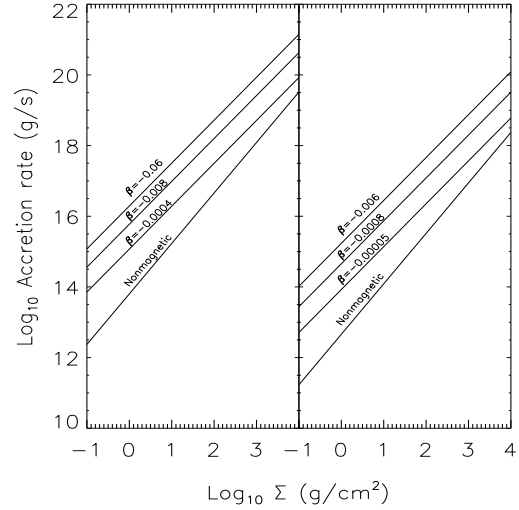
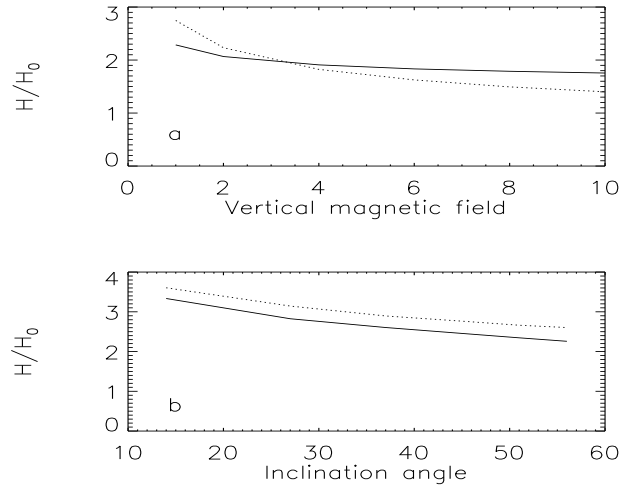
**Figure 3.** The magnetic-disc accretion rates (normalized with accretion rates without magnetic fields) as a function of **a)** the vertical field B^{vert} for $\alpha_{SS}=0.01$, $\beta = -2 \cdot 10^{-3}$ (solid) and $\Sigma = 1.4 \text{ g/cm}^2$ (dotted); **b)** the inclination angle i for $B^{\text{vert}} = 1$, $\alpha_{SS}=0.1$ (solid), $\alpha_{SS}=0.01$ (dotted). Ψ is defined by (41). $Pm=1$

small i (the last case is the same as the case with large B^{vert} when $\hat{\Sigma}$ fixed).

Due to the direct relation between accretion rate and surface density (Fig. 4) the dimensionless surface density dependence on parameters is the same as for the dimensionless accretion rate. The surface density for magnetic discs is usually smaller than for nonmagnetic discs for the same accretion rate. The magnetic disc radial velocity is greater than nonmagnetic disc radial velocity (the accretion rate is greater in magnetic disc). The surface density does not depend on α_{SS} because the toroidal magnetic field is always small and we can neglect its influence on the pressure.

4.2 Disc thickness

In Fig. 5 the thickness for magnetic discs is shown in comparison to the nonmagnetic case. The magnetic disc is thicker than the nonmagnetic one for all calculated models. Never-

**Figure 4.** The accretion rate as a function of the surface density Σ for $\alpha_{SS} = 0.1$ (left) and $\alpha_{SS} = 0.01$ (right). The numbers are given in Table 1. $Pm=1$, $B^{\text{vert}} = 1$ **Figure 5.** The magnetic-disc height in comparison with nonmagnetic-disc height as a function of **a)** the vertical magnetic field B^{vert} . $\beta = 2 \cdot 10^{-3}$ (solid) and $\dot{M} = 4 \cdot 10^{16} \text{ g/s}$ (dotted), $\alpha_{SS}=0.01$; **b)** the inclination angle i for $\alpha_{SS}=0.1$ (solid), $\alpha_{SS}=0.01$ (dotted). $Pm=1$, $B^{\text{vert}} = 1$

theless, this fact is only a rule with exceptions. Note that magnetic discs can be thinner than nonmagnetic discs for both large B^{vert} and Pm . However, we should care the radial flow Mach number. The radial flow can become supersonic for $H < H_0$ for large enough α_{SS} . This problem completely disappears for small α_{SS} . The disc thickness decreases with increasing radial magnetic field and vertical magnetic field due to magnetic stresses (see Fig. 5). It is interesting to note that the accretion rate is getting larger for thinner disc. The disc thickness weakly depends on Pm as well as α_{SS} .

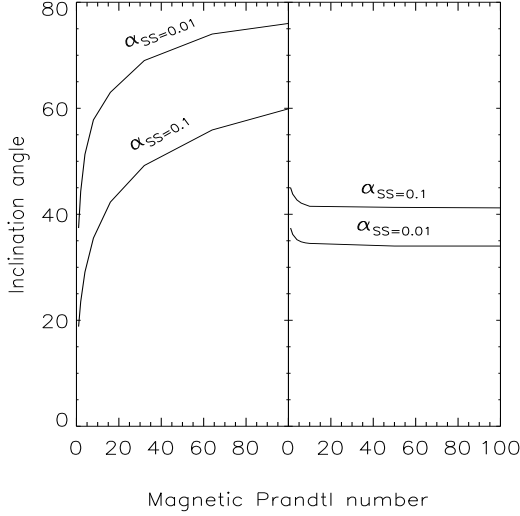


Figure 6. The inclination angle i of magnetic field lines to the rotation axis for $B^{\text{vert}}=1$. **LEFT:** toroidal field fixed ($\beta = -9 \cdot 10^{-4}$), **RIGHT:** column density fixed $\Sigma = 1.4 \text{ g/cm}^2$

4.3 Inclination angle i

We find that for rather low β the inclination angle i can be larger than the critical value of 30° (Blandford & Payne 1982) for jet launching even for Pm of order unity. This result is in accordance with our calculation for polytropic magnetic disc (paper I). Moreover, for given surface density the inclination angle hardly depends on Pm (Fig.6) also in accordance with the results of paper I. This means that the radial velocity is proportionate to $1/\text{Pm}$ in this case. Nevertheless, the inclination angle depends strongly on Pm for given accretion rate. The inclination angle increases for decreasing α_{SS} for fixed accretion rate and decreases for fixed surface density. Such a behaviour is the result of the behaviours of accretion rate and surface density with changing α_{SS} .

According to (35) and (25), the accretion rate is connected with β . So, for given B^{vert} there is a direct relation between the β and the resulting inclination angle i , Table 1 presents the numbers. Our model yields high accretion rates and high inclination angles already for rather small β . The larger the β is the higher the i . According to (1), the β increased inwards. We can conclude that the Blandford-Payne condition is fulfilled most easily for the inner part of the accretion disc.

5 CONCLUSION

The vertical structure of accretion discs with an imposed vertical magnetic field has been considered. The magnetic field energy is supposed as to be in balance with the accretion flow energy. The angular momentum transport is fully provided by the magnetic field, the Reynolds stress does here not play any role.

The turbulent viscosity might only be important for the energy balance of the disc but the calculations demonstrated also the dominance of the Joule heating. The magnetic field is, therefore, the essential feature of the model and the equations do not change to standard α -disc equations in the small

magnetic field limit. Stehle & Spruit (2001) results is also confirmed the existence of magnetic field induced accretion. The results actually demonstrate the close relation between magnetic field dragging and the vertical structure of thin accretion disc. The interaction of the magnetic field with the disc can drastically change the disc structure as well as the configuration of the magnetic field. The angular velocity differs from the Keplerian one. This difference is, however, relatively small because the magnetic energy is small compared with the gravitational energy in our model. The radial velocity, however, can increase drastically becoming comparable to the sound speed for some models. This can lead to a strong amplification of the accretion rate for a given column density (Fig.4).

The accretion rate is connected directly with the surface toroidal magnetic field in our model. Nevertheless, even small toroidal magnetic field at the surface ($\beta \ll 1$) is enough to increase the accretion rate drastically. The accretion rate can be as amplified drastically (large i and small Pm), so suppressed (small i and large Pm).

The magnetic disc is basically thicker than the nonmagnetic one for typical parameters values. Nevertheless, we can not exclude that the magnetic disc can become thinner than a nonmagnetic one for some parameters (e.g. large B^{vert}).

However, the most surprising results of our calculations concern the inclination angle i of the magnetic field lines to the rotation axis. We found that i) already rather small toroidal field component B^{tor} can produce inclinations exceeding the critical value of 30° and ii) this effect is almost independent of the magnetic Prandtl number for given surface density Fig. (5).

In previous studies (Lubow, Papaloizou & Pringle 1994; Reyes-Ruiz & Stepinski 1996) large radial inclinations could only be obtained for $\text{Pm} \geq 100$. After our results it also holds for $\text{Pm}=1$. The difference is due to the fact that the previous studies neglect the magnetic field influence on disc structure and used radial velocity from standard accretion disc theory.

For a given accretion rate, \dot{M} , the larger β lead to the larger i and to the smaller Σ (Fig. 4). As after (1) the larger (negative) β exist in the innermost accretion disc region, we have there the smaller column density and the stronger radial inclination of the field lines. The jet launching should thus be concentrated to the inner region of an accretion disc.

Only Kramers opacity was used in this paper but it might be very interesting to apply other opacity laws to reformulate the stability problem of the structure of accretion discs.

Acknowledgements: D.S. thanks for the kind financial support by the Deutsche Forschungsgemeinschaft and Russian foundation for basic research (grant RFBR-DFG 00-02-04011). G.R. acknowledges the kind hospitality of the HAO during the work on this paper.

REFERENCES

- Bardou A., Heyvaerts J., 1996, A&A, 307, 1009
- Blandford R.D., Payne D.G., 1982, MNRAS, 199, 883
- Brandenburg A., Campbell C.G., 1998, MNRAS, 298, 223

- Campbell C.G., 1997, *Magnetohydrodynamics in binary stars*.
Kluwer, Dordrecht
- Campbell C.G., 1998, MNRAS, 301, 754
- Campbell C.G., Heptinstall P.M., 1998a, MNRAS, 299, 31
- Campbell C.G., Heptinstall P.M., 1998b, MNRAS, 301, 558
- Elstner D., Rüdiger G., 2000, A&A, 358, 612
- Krasnopolsky R., Li Z.-Y., Blandford R., 1999, ApJ, 526, 631
- Kluzniak W., Kita D., 2000, astro-ph/0006266.
- Livio M., Pringle J.E., 1992, MNRAS, 259, 23
- Lubow S.H., Papaloizou J.C.B., Pringle J.E., 1994, MNRAS, 267, 235
- Lynden-Bell D., 1996, MNRAS, 279, 389
- Ogilvie G.I., 1997, MNRAS, 288, 63
- Ogilvie G.I., Livio M., 1998, ApJ, 499, 329
- Ouyed R., Pudritz R.E., 1999, MNRAS, 309, 233.
- Regev O., 1983, A&A, 126, 146.
- Reyes-Ruiz M., Stepinski T.F., 1996, ApJ, 459, 653
- Press W.H., Teukolski S.A., Vetterling W.T., Plannery B.P., 1992,
Numerical recipes in C. The art of scientific computing. Cam-
bridge Univ. Press.
- Shakura N.I., Sunyaev R.A., 1973, A&A, 24, 337
- Shalybkov D., Rüdiger G., 2000, MNRAS, 315, 762 (Paper I)
- Stehle R., Spruit H., 2001, astro-ph 0103409
- Ustyugova G.L., Koldoba A.V., Romanova M.M., Chechetkin
V.M., Lovelace R.V.E., 1999, ApJ, 516, 221